

Document downloaded from:

<http://hdl.handle.net/10251/83533>

This paper must be cited as:

Pacheco-Paramo, DF.; Akyildiz, IF.; Casares Giner, V. (2016). Local Anchor Based Location Management Schemes for Small Cells in HetNets. IEEE Transactions on Mobile Computing. 15(4):883-894. doi:10.1109/TMC.2015.2431717.



The final publication is available at

<http://dx.doi.org/10.1109/TMC.2015.2431717>

Copyright Institute of Electrical and Electronics Engineers (IEEE)

Additional Information

(c) 2015 IEEE. Personal use of this material is permitted. Permission from IEEE must be obtained for all other users, including reprinting/ republishing this material for advertising or promotional purposes, creating new collective works for resale or redistribution to servers or lists, or reuse of any copyrighted components of this work in other works.

Local Anchor Based Location Management Schemes for Small Cells in HetNets

Diego Pacheco-Paramo, Ian F. Akyildiz, *Fellow, IEEE*,
and Vicente Casares-Giner, *Member, IEEE*

Abstract—Existing location management (LM) methods for macrocells in LTE-Advanced have tracking area list (TAL) granularity. Therefore, a user equipment (UE) triggers a location update (LU) whenever it leaves its current TAL, and it is searched through paging (PG) with TAL accuracy. However, these procedures are not well-suited for small cells (SCs). The reasons are twofold. First, dense deployments of SCs imply that paging has a low probability to be successful in the first attempt, increasing the signaling overhead in the Core Network (CN). Second, smaller coverage areas lead to a higher mobility among cells, increasing the signaling overhead in the CN due to LUs. In this work, two LM schemes with fine granularity are proposed. These schemes update UE's location to a local anchor (LA) in a SC or tracking area (TA) basis, respectively. By increasing the accuracy of UE's location, a significant reduction of signaling overhead in the CN due to PG is achieved. Moreover, LUs to the LA are performed through direct X2-interface links to avoid signaling overhead in the CN. A versatile mobility model is developed and closed-form expressions for UEs' mobility metrics are found to validate the proposed schemes through variations of critical parameters such as TA/TAL configuration, UE's mobility patterns and cell residence times.

Index Terms—Location management, small cells, paging, location update, tracking area list.

1 INTRODUCTION

SMALL cells (SCs) play a crucial role towards satisfying the capacity requirements imposed on mobile networks [1] [2]. Moreover, it is expected that they scale properly in order to effectively enhance performance in dense indoor/outdoor scenarios [3]. Likewise, the success of large-scale deployments depends on their ability to coordinate and optimize their resources while avoiding additional processing load on current networks. Some of the issues that have been identified and addressed in SC networks are interference avoidance, cell search, cell selection and handover decision/execution. However, there is not sufficient research carried out in solving the issues that make location management methods of macrocells unsuitable for small cells. Two characteristics of SCs have been identified to have a negative impact in macrocell location management methods: (i) backhaul

restrictions, and (ii) small coverage areas. The former imposes a tighter bound on signaling overhead, since the backhaul is shared with fixed users. The latter implies that users cross cells more often, and therefore more signaling is required per user.

Location management involves two key procedures: location update (LU) and paging (PG). LUs are triggered by the User Equipment (UE) to inform about its current position to the Mobility Management Entity (MME) in the Evolved Packet Core (EPC). To that purpose, the 3GPP standard defines three levels on which to locate a UE: (i) cell level, (ii) tracking area (TA) level, and (iii) tracking area list (TAL) level. A cell is the minimum unit of coverage for UEs. A TA is a group of cells that share a TA identifier (TAI) and each cell belongs to only one TA. A TAL is a UE specific set of TAs where the UE can camp without triggering an LU procedure. Once a UE camps in a cell with a TAI that does not belong to its TAL, it triggers an LU procedure, referred to in the standards as a Tracking Area Update (TAU) procedure. With this procedure, the MME is informed that the UE has left the current TAL. Then, the MME responds with the assignment of a new TAL to the UE [4].

A paging procedure starts when an incoming call has to be routed to a UE. Since the MME knows the

- D. Pacheco-Paramo was with Broadband Wireless Networking Lab, Georgia Institute of Technology, Atlanta, GA, 30332, USA. Now he and V. Casares-Giner are with Universitat Politècnica de València, Camino de Vera, s/n, 46022, Valencia, Spain. e-mail:(diepacpa@posgrado.upv.es and vcasares@dcom.upv.es).
- I. Akyildiz is with the Broadband and Wireless Networking Laboratory, School of Electrical and Computer Engineering, Georgia Institute of Technology, Atlanta, GA 30332 USA. e-mail:(ian@ece.gatech.edu).

UE location in a TAL granularity, the UE is searched in the cells of the current TAL. The basic paging policies can be classified as parallel and serial [5]. In parallel paging, also named as non-selective or blanking paging, the UE is simultaneously searched in all the cells that belong to the TAL. In serial paging, also named as selective paging, the UE is searched sequentially, for instance, according to certain estimated probability of determining the UE in a given area [6], according to the distance to the cell in which the UE had its last contact with the network [7] or according to the location granularity of the UE [8]. For example, in [8], three policies are proposed and evaluated, two of them labeled as Cell-TAL and TA-TAL, a two-step searching scheme, and the other scheme labeled as Cell-TA-TAL, a three-step scheme.

There is a tradeoff between LU and PG costs. As LUs are performed more often, the amount of paging is reduced and vice-versa. For instance, as the size of the TAL grows, the UE will cross less TALs, hence reducing the LUs, but more cells have to be paged. From an operator's point of view, TA's setting has a higher cost than TAL's setting, since adding or discarding cells from a TA involves equipment reconfiguration, which forces service interruption for the cells involved. Hence, in order to successfully adapt to traffic conditions, most of the existing work focus on TAL configuration. In [9], while TA size remains fixed, TAL size is dynamically changed according to the user's speed. This allows for high speed users to reduce their TAUs by using bigger TALs. However, this solution requires the introduction of specific timers for each user in the MME, which increases its complexity and implementation cost. In [10], the TAL design approach is proved to be more effective than the TA design approach to reduce signaling overhead, assuming that the load of cells and handover data is available from the network, and that this information is enough to construct traces that correctly represent users' movements. A more direct approach consists in analyzing location patterns obtained from Call Data Records (CDRs) in order to identify the most frequently visited areas and correlate this information with the service provided to the user or the underlying structure of the area, which could be used to design effective paging schemes [11],[12]. Yet, since user-profile based schemes define a subset of cells for a first paging cycle according to historical information, a proportion of users will inherently suffer from paging delay.

One of the main concerns in TA/TAL design is to reduce the impact that TAUs and PG signaling overhead have over the EPC, and in particular over the MME. According to [13], 34% of the processing load in the MME is due to LM procedures, where 29%

is due to paging and 5% is due to TAUs, and it is expected that these values grow with the introduction of SCs. An important processing load reduction in the MME may be achieved through direct cell interaction. In [14] a PG procedure that forwards PG messages from cell to cell is proposed. These messages are sent through the X2 interface [15], which has been defined in 3GPP as a logical link to support direct interaction among cells. However, routing through one-hop steps rapidly increases the load in SCs' backhaul for large deployments.

There are two main contributions in our work. First, we propose two location management schemes for small cells that achieve a finer granularity of UE's location by registering its position in a SC or TA basis to a Local Anchor (LA). LA-based solutions have already been proposed to reduce excessive signaling associated to high mobility in cellular networks. In [16], a VLR is chosen as an LA, reducing the registration frequency to the HLR. However, in that solution the LA remains inside the Core Network, and hence the communication among LAs increments the signaling load of the Core Network (EPC for 3GPP). In our work, the LA is chosen among the SCs, and in order to avoid increasing the signaling load in the EPC, location updates among SCs are performed through direct links using the X2 interface. For scalability purposes, an X2 Router [17] is used, so each SC only has to maintain a single X2 connection. On the other hand, the LA is chosen on a per-user-basis from all the SCs in the TAL, distributing the processing load. More importantly, by achieving a finer granularity of the UE location, the processing load associated with paging in the MME is considerably reduced.

Second, we use a versatile mobility model to validate our LA-based LM schemes in relevant scenarios and provide closed-form expressions for LM metrics. These scenarios include variations of TA's and TAL's sizes and shapes, cell residence times, UE's mobility patterns and mobility adaptive TAL configuration policies.

The rest of this document is organized as follows. In section 2, we review the 3GPP solution for location management. In section 3 we introduce our two proposed local anchor based location management procedures and describe their associated signaling. In section 4, we describe the mobility model of UEs, the configuration of TALs, and find closed-form expressions for relevant LM metrics. Then, in section 5 we use these expressions to define the signaling cost functions of the 3GPP scheme and our two proposed LM schemes. The total signaling cost of the two proposed schemes and the 3GPP solution are compared in section 6. Finally, section 7 concludes the paper.

2 RELATED WORK: 3GPP-BASED SCHEME

The location management procedure in 3GPP groups cells into Tracking Areas (TA) where each cell can belong to only one TA. In the same way, a Tracking Area List (TAL) is a group of TAs where a UE can camp without triggering a TAU. These TALs are defined on a per-user basis and set the granularity to which users' location is known. In Fig. 1 we show a deployment of 7 SCs grouped in TAs to describe the location management procedure of 3GPP. The correspondence of SCs and TAs is as follows: $TA\ 1 = \{SC\ 1, SC\ 2\}$, $TA\ 2 = \{SC\ 3, SC\ 4, SC\ 5\}$ and $TA\ 3 = \{SC\ 6, SC\ 7\}$. Each TA has a unique Tracking Area Identifier (TAI) which is broadcasted by the SCs. Let us consider the UE camping in SC 1 and moving to SC 6 following the route $A-B-C$. Originally, this UE has TAL x , which is composed of TA 1 and TA 2. In transition C , after SC 6 broadcasts its TAI, the UE looks for this TAI in its TAL, and a Tracking Area Update (TAU) is performed since SC 6 does not belong to TAL x . This TAU procedure has a twofold purpose: First, it informs the MME of the UE location. Second, the MME delivers a new TAL to the UE, in this case TAL y . In order to reduce the signaling associated with the ping pong effect [18][19], the last visited TA after a TAU procedure is part of the new TAL. Therefore, TA 2 belongs to both TAL x and TAL y . An important consequence of the TAU procedure is that paging is done on a TAL-basis. For example, if a user is following the same route $A-B-C$, and a call arrives just after the transition in B , the MME only knows that the user is inside TAL x , and the UE will be searched according to that information.

In Fig. 1, the relevant elements of the EPC for LM are displayed. The Mobility Management Entity (MME) is responsible for the LM functions such as tracking, paging and setting of TALs for UEs. It also decides if during a TAU procedure it is necessary to change the Serving Gateway (SGW). The SGW is responsible for data transfer to UEs. The Packet Data Network Gateway (PDN GW) needs to maintain recent information about each UE corresponding MME and SGW in order to connect to the PDN. The Home Subscriber Server (HSS) is responsible for registering UEs, including information about its current MME. Finally, the Home eNodeB GW (HeNB GW) is the point where the SCs (defined as HeNBs in 3GPP) connect to access the EPC.

Four variations of the TAU procedure are defined in the standards [4], differing in the use of the elements of the EPC. The most common and simplest type of TAU procedure only involves the MME in the EPC, as shown in Fig. 2, and is the one used as reference in this work.

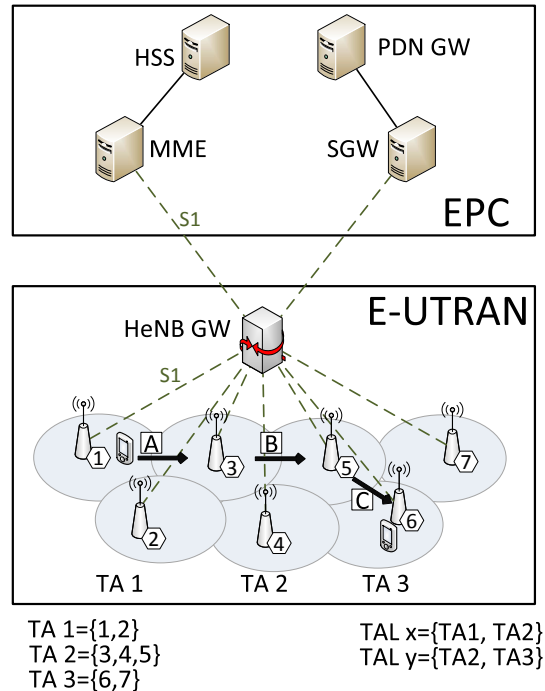


Fig. 1: Tracking Area Update procedure and elements in the Evolved Packet Core.

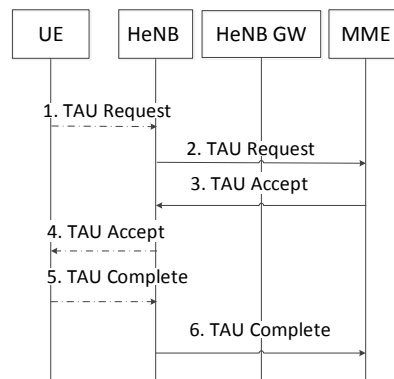


Fig. 2: Tracking Area Update procedure in 3GPP.

The signaling associated with a single paging procedure is described in Fig. 3. For the 3GPP-based solution used throughout this work for reference purposes, we will consider the PG scheme CT (TA-TAL) [8], that achieves a good performance while maintaining compatibility with the 3GPP standard. In this PG scheme, when a call is addressed to the UE, the MME will page the last TA to which the last contacted SC belongs. If it fails, all the remaining cells of the TAL will be paged.

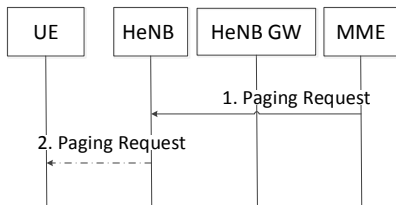


Fig. 3: Paging procedure in 3GPP.

3 PROPOSED LOCAL ANCHOR BASED SCHEMES

We utilize SCs as Local Anchors (LAs) that register the position of UEs inside a TAL using the X2 interface [20]. By means of introducing LUs for movements of UEs inside the TAL, we achieve a finer granularity of their location, and thus reduce the signaling overhead associated to paging in the MME.

In our proposed LA-based schemes, as a UE enters the ECM-idle mode, which means that the user is registered to the network but is not active, a three-step sequence is followed: First, the UE registers its position to the MME. Then, the MME sends a TAL to the UE. Finally, the UE registers its position to the LA in the TAL. Let us recall that the first two steps are part of the TAU procedure described in section 2. The last step, defined as a location update to the local anchor, is introduced in this work and can be performed separately from the first two. Any SC can be an LA, and this element is responsible for keeping track of its registered UEs. Additionally, the LA is defined on a per-user-basis, which allows to distribute the signaling load generated by UEs among the SCs in the network.

Location updates to the LA are performed through the X2 interface without intervention of the EPC, thus avoiding signaling overhead in the MME. As can be seen in the architecture of Fig. 4, an X2 Router is included in the E-UTRAN [17]. This X2 Router can co-exist with the HeNB GW since it only affects the X2 link and its main function is to maintain an X2 link among the SCs through a single connection. This is convenient for scalability purposes and also to allow X2 connectivity to macrocells.

Our two LA-based schemes differ in their location granularity. The LA-based scheme with SC granularity sends LUs to the LA every time a UE crosses a SC inside the TAL. On the other hand, the LA-based scheme with TA granularity only sends LUs to the LA when a TA inside the TAL is crossed. Let us recall that both schemes are compliant with the 3GPP standards, since the TAU procedure described in Section 2 is

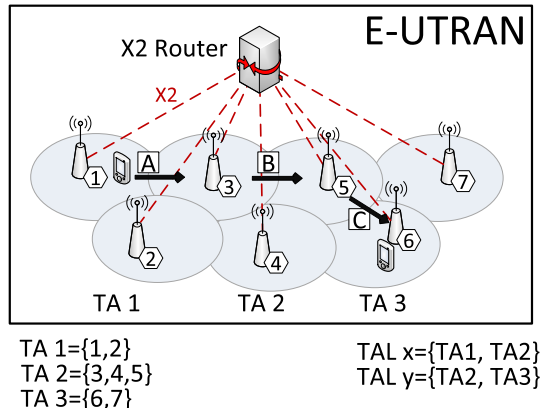


Fig. 4: E-UTRAN architecture for LU and Paging in LA-based schemes.

still performed when the UE leaves its TAL. The LU signaling to the Local Anchor is described in Figure 5. First, the destination SC receives an LU request from the UE, with information about its current LA. Then, the SC forwards this message to the LA through the X2 Router. It can be observed that it is fairly simple though it implies the participation of three elements: (i) destination SC, (ii) X2 Router and, (iii) Local Anchor.

The paging procedure for the LA-based schemes is described in Figure 6. First, the MME pages the last registered SC in the TAL, that is, the current LA of the UE. This procedure is done according to the 3GPP standard, using the S1 interface. Then, the LA forwards the paging request to the X2 Router with information about the destination SC or TA. The X2 Router then forwards the paging request to the corresponding SC or TA. Although this procedure involves more steps than the 3GPP-based solution described in Figure 3, the total paging signaling is reduced by having precise information about the location of UEs.

3.1 Local Anchor Based Scheme with Small Cell Granularity

In our first proposed scheme, LA-SC, a UE will send Location Updates (LU) to the LA through the X2 interface on a SC-basis. Therefore, each time a user hops from one SC to another, an LU message is sent to the LA, which will keep a record of the last visited cell. In Fig. 4, a UE is originally placed in SC 1 and follows the route *A-B-C*. Since SC 1 is the first SC where the UE is registered, it is chosen as its LA. The UE sends an LU message to SC 1 just after the transitions in *A* and *B*, notifying that the new visited SC is, respectively SC 3 and SC 5. Beyond *C*, the UE triggers a TAU procedure,

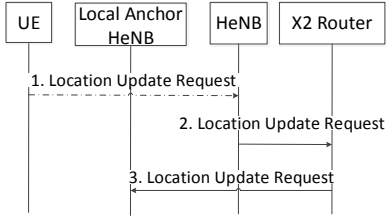


Fig. 5: Location update to the local anchor through the X2 interface.

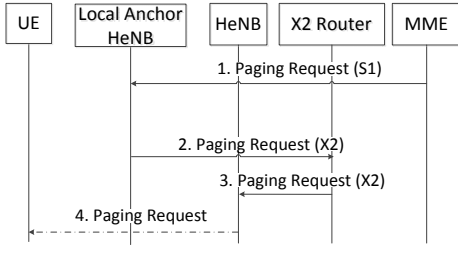


Fig. 6: Paging using the local anchor through the X2 interface.

and also SC 6 is chosen as the new LA. Therefore, signaling is sent to the E-UTRAN only in C . If the UE receives a call just after B , the LA, i.e. the SC 1, receives the paging message through the S1 interface, and forwards it to the current SC (SC 5) through the X2 Router. Therefore, with this scheme, the UE is tracked at SC level, that is, it offers the finest granularity (1 SC).

3.2 Local Anchor Based Scheme with Tracking Area Granularity

In our second proposed scheme, LA-TA, a UE will perform LUs to the LA through the X2 interface in a TA-basis. In this case, when the user hops from one TA to another inside its TAL, an LU message indicating the new TAI is sent to the LA. Let us consider a UE originally placed in SC 1 that follows the route A - B - C as shown in Figure 4. The chosen LA is the same as in the previous scheme. However, the UE only sends an LU message to the LA in A , but not in B , and then in C a TAU procedure is triggered. If a call is forwarded to the UE after B , the LA will only know its current TA, and therefore all the SCs inside TA 2 will be forwarded the paging message through the X2 Router. Notice that, in both the proposed schemes, after leaving the former TAL x , the UE has to change the LA to the first visited SC in the new TAL y , SC 6.

4 MOBILITY MODEL DESCRIPTION AND METRICS ESTIMATION

In this section, we provide an analytical approach to assess the impact of mobility in the performance of LM schemes. To that purpose, we first revisit a 2D mobility model for UEs in a small cell network. Then, based in the proposed cell layout, we define the structure of TAs and TALs, and present two mobility-dependent TAL configuration solutions. Finally, we obtain closed-form expressions for three metrics that determine the signaling cost of LM procedures: (i) the mean number of location update messages to a local anchor, (ii) the mean number of Tracking Area Update procedures to the MME, and (iii) the probability of finding a UE in a given SC.

4.1 Mobility and Traffic Model

As in [21], here we use a 2D versatile mobility model. First, the sojourn or the residence time of a UE in a SC is defined by a Gamma distribution [8], with Laplace transform $f_m^*(s)$ given by:

$$f_m^*(s) = \int_0^\infty f_m(e)e^{-st} dt = \left(\frac{\lambda_m \gamma}{s + \lambda_m \gamma} \right)^\gamma, \quad (1)$$

where the mean and variance are respectively given by $1/\lambda_m$ and $1/(\gamma\lambda_m^2)$. It make sense to consider the Gamma distribution as cell residence time since it has been used in many studies about location management [35].

Second, we assume a 2D tessellation of regular hexagons. This model allows us to evaluate the proposed solutions in large-scale, dense small cell deployments, as can be expected in urban areas of cities such as New York, Chicago or Boston, where users tend to remain inside clusters of small size (1-3 km²) that account for a significant amount of their traffic volume (30%-50%)[12]. To serve these extended hotspots for indoor/outdoor scenarios, microcells and metrocells are appropriate [22],[23]. These types of small cells have high capacities and coverage areas that can go from 100 m to 2 km.

According to the proposed tessellation, once the UE leaves a SC, it can move in 6 different directions as shown in Figure 7. The transition probabilities are a function of the parameter α and an orientation as it is shown in Table 1, where a normalization factor $D(\alpha) = 1+2\alpha+2\alpha^2+\alpha^3$ is included, [21]. By defining an orientation and choosing an appropriate value of α it is possible to increase the probability of going in any direction. For example, by choosing orientation 1 and setting $\alpha > 1$, the UE will have a higher probability of going to North (N). On the other hand, if $\alpha < 1$, the UE will have a higher probability of going to South

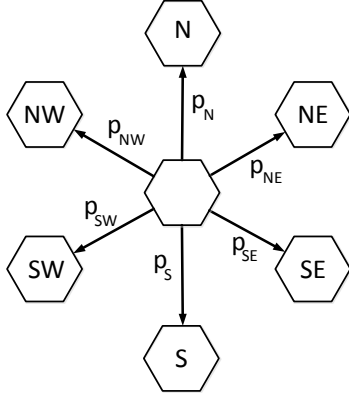


Fig. 7: Transition probabilities for each direction.

TABLE 1: Transition probabilities, $D(\alpha)=1+2\alpha+2\alpha^2+\alpha^3$.

	Orientation 1	Orientation 2	Orientation 3
$p_N(\alpha)$	$\alpha^3/D(\alpha)$	$\alpha^2/D(\alpha)$	$\alpha/D(\alpha)$
$p_{NE}(\alpha)$	$\alpha^2/D(\alpha)$	$\alpha^3/D(\alpha)$	$\alpha^2/D(\alpha)$
$p_{SE}(\alpha)$	$\alpha/D(\alpha)$	$\alpha^2/D(\alpha)$	$\alpha^3/D(\alpha)$
$p_S(\alpha)$	$1/D(\alpha)$	$\alpha/D(\alpha)$	$\alpha^2/D(\alpha)$
$p_{SW}(\alpha)$	$\alpha/D(\alpha)$	$1/D(\alpha)$	$\alpha/D(\alpha)$
$p_{NW}(\alpha)$	$\alpha^2/D(\alpha)$	$\alpha/D(\alpha)$	$1/D(\alpha)$

(S). To increase the probability of going to the other directions, we have to choose orientation 2 or 3. It should be noted that random-walk can be achieved by setting $\alpha = 1$. Also, notice that $p_N(\alpha) = p_S(\alpha^{-1})$, $p_{SE}(\alpha) = p_{NW}(\alpha^{-1})$, and $p_{SW}(\alpha) = p_{NE}(\alpha^{-1})$.

As traffic model, call arrivals to the UEs follow a Poisson process with rate λ_c .

4.2 Tracking Area List Configuration

We present two TAL configuration policies. The central policy TAL configuration aims to reduce the TAUs caused by the ping-pong effect. The adaptive policy TAL configuration is our proposal, and aims to reduce the TAU frequency by choosing a TAL that maximizes the sojourn time for a given UE mobility pattern.

4.2.1 The Central Policy TAL Configuration

Let us consider a large deployment of SCs covering hexagonal areas as shown in Figure 8. Each TA is composed of S_{TA} SCs and each TAL is composed of S_{TAL} TAs. In this case, each TA is surrounded by a blue line, and is composed of 3 SCs, hence $S_{TA} = 3$. In other words, a TA adopts the mosaic graph M_0 structure, [24]. Let us define that TAL 1 is composed of {TA 1, TA 2, TA 3, TA 4, TA 5, TA 6, TA 7}, ($S_{TAL} = 7$), that is, one TA surrounded by 6 TAs and is represented by the TAs inside the red line in Figure

8. Notice that this structure looks like a mosaic graph T_1 [24]. With the objective of reducing the signaling associated to the ping-pong effect, TALs overlap [25]. The ping-pong effect more likely occurs when a UE moves in a random way. For example, in our mobility model, this corresponds to α values around 1. If a UE with TAL 1, moves from TA 6 to TA 9, a TAU procedure is performed as explained in the previous section. The new TAL contains the last visited TA (TA 6) and positions the new visited TA (TA 9) as close to the center of the new TAL as possible. Therefore TAL 2 is composed of {TA 6, TA 7, TA 8, TA 9, TA 10, TA 12, TA 13} and it is represented by the TAs inside the green line. If the UE in TA 9 goes back to TA 6, it remains with TAL 2, since TALs overlap and TA 6 belongs to both TAL 1 and TAL 2. This centralized scheme, or *central policy*, has been proposed and studied by several authors to reduce the frequency of TAU (or LUs) messages when a random-walk model is considered as it is shown, for instance, in [4], [18], [26], [27], and [28]. When an incoming call is delivered to the UE, that is, after a successful paging, a TAL update is also performed. In this case, the assignment of the new TAL also follows the central policy.

4.2.2 The Adaptive Policy TAL Configuration

We consider the same SCs deployment shown in Figure 9, with $S_{TA} = 3$, $S_{TAL} = 7$ where the UEs' move in the North-East (NE) direction with a higher probability than any other directions, i.e., orientation 2 and α significantly higher than 1, see Table 1. This scenario represents UEs' following a restricted path, e.g., a group of vehicles moving in a highway [29]. In this case, the ping-pong effect will occur less frequently and the central policy TAL configuration may not be a suitable solution. An intuitive approach is to perform the assignment of the starting SC in the new TAL in such a way that the sojourn or residence time in this new TAL be maximum; equivalently to minimize the rate of TAU [27]. As an example, Figure 9 shows the resulting new TAL when the UE leaves from TA 6 in direction NE and is composed of {TA 8, TA 9, TA 11, TA 12, TA 13, TA 14, TA 15}, that is, there is no overlapping with the previous TAL. We call this the adaptive TAL configuration or *adaptive policy* and basically deals with the estimation of the SC and TA that the UE should begin in the new TAL. Obviously, the assignment of the starting SC must be in agreement with the 2D geographical cell layout. With this regard, a significant advantage of this approach is that it uses already defined TAs, which is convenient since the cost of configuring new TAs is higher than that of configuring TALs. As in section 4.2.1, when an incoming call is delivered to the UE,

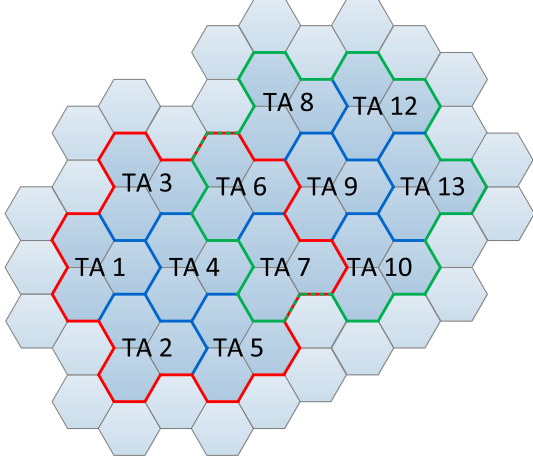


Fig. 8: Central Tracking Area Lists configuration with $S_{TA}=3$, $S_{TAL}=7$. Suitable for random-walk model, $\alpha=1$.

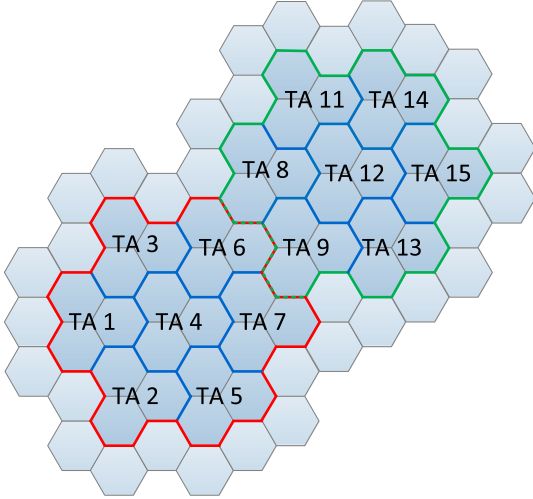


Fig. 9: Adaptive Tracking Area Lists configuration with $S_{TA}=3$, $S_{TAL}=7$. Suitable for $\alpha > 1$.

that is, after a successful paging, a TAL update based on central policy is also performed.

4.3 Location Management Metrics Estimation

We utilize the proposed mobility model and the TAL configuration policies to obtain closed-form expressions for the mobility metrics that define signaling in location management. These are obtained as follows.

4.3.1 Mean Number of Tracking Area Updates to the MME

The SC's residence or sojourn time of a UE follows a Gamma distribution and when exiting a given SC, the

UE visits one of the six neighboring SCs according to the routing probabilities of Table 1. A Tracking Area Update (TAU) message is sent by the UE every time it leaves the TAL. Figure 10(a) shows a SC network with $S_{TA} = 3$ and $S_{TAL} = 7$. The 21 SCs inside the TAL and the 21 SCs that are external, surrounding and adjacent to the TAL, are enumerated. Following Appendix A, the TAU messages can be seen as a point process characterized by a Markovian Arrival Process (MAP). Then, matrix \mathbf{D}_0 contains the transition probabilities between SCs that belong to the TAL where the UE is actually roaming. Matrix \mathbf{D}_1 contains the exiting transition probabilities from the TAL towards the adjacent SCs plus the entering transitions from the adjacent SCs towards SCs of the new TAL. In other words, the adjacent SCs to the current TAL are ephemeral states in the MAP, which means that immediately after the UE is absorbed in one of the 21 adjacent states, an instantaneous transition towards one of the SCs of the new TAL follows. Therefore, the transitions of \mathbf{D}_0 do not involve TAL updates, while the transitions of \mathbf{D}_1 do.

So, the dynamics of the UE is modeled with a semi-Markov process characterized by a discrete-time Markov chain (DTMC) with stochastic matrix $\mathbf{\Pi} = \mathbf{D}_0 + \mathbf{D}_1$, see Appendix A. Figure 10(b) shows the same deployment as Figure 10(a), in which the adjacent states have been re-enumerated according to the position that the UE will occupy initially in the new TAL. This strategy corresponds to the *central policy*. In other words, after exiting the current TAL, the UE sets its new position in one of the three SCs of the central TA, in SC 0, SC 1 or SC 2. It is important to recall that \mathbf{D}_1 takes into account the SC at which the UE starts remaining in the new TAL.

Following the example of Figure 10, notice that when the mobility model is not random-walk ($\alpha \neq 1$), the *adaptive policy* could be a better solution than the *central policy*. In this case, the starting TA could be one of the other six TAs around the central TA. Then, the surrounding SCs with number 0 in Fig.10(b), could be replaced by 3, 6, 9, 12, 15 or 18 and the surrounding states numbered with 1 and 2, could be replaced by, respectively, 4, 7, 10, 13, 16 or 19 and 5, 8, 11, 14, 17 or 20.

According to the results (27) obtained in the Appendix A, the mean number of TAU messages triggered by the UE, \bar{N}_{TAU} is given by

$$\begin{aligned} \bar{N}_{TAU} &= \mathbf{P}_{isc} \sum_{z=0}^{\infty} \beta(z) \mathbf{M}^{(z)} \\ &= \mathbf{P}_{isc} f_{m,r}^*(\lambda_c) [\mathbf{I} - f_m^*(\lambda_c) \mathbf{\Pi}]^{-1} \mathbf{D}_1 \mathbf{e}, \quad (2) \end{aligned}$$

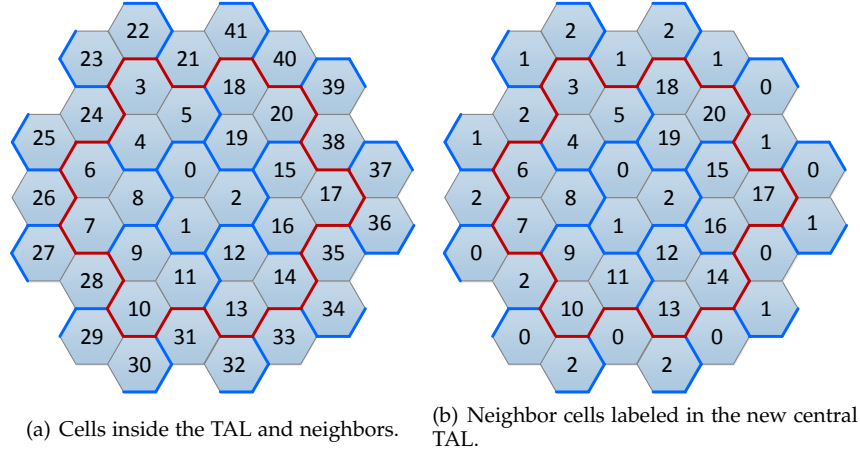


Fig. 10: Diagram to calculate \bar{N}_{TAL} for $S_{TA}=3$ and $S_{TAL}=7$

where \mathbf{P}_{isc} is a vector containing the probabilities of finding a UE in each SC of a TAL just immediately after the reception of the last incoming call, $\beta(z)$ is the probability that a UE performs z SC transitions between two call arrivals, and $\mathbf{M}^{(z)}$ is the mean number of TAUs in z SC transitions, see Appendix A.3 .

4.3.2 Mean Number of Location Updates to the Local Anchor

In the LA-SC Based scheme, a Location Update is sent to the Local Anchor (LA) every SC crossing that does not involve a TAU procedure. Clearly, the mean number of LUs to the LA $\bar{L}\bar{U}_{LA-SC}$ is, from (2)

$$\bar{L}\bar{U}_{LA-SC} = \frac{1}{\theta} - \bar{N}_{TAU}, \quad (3)$$

where the parameter $\theta = \lambda_c/\lambda_m$ is the call-to-mobility ratio.

In the LA-TA Based Scheme, a Location Update is sent to the LA every TA crossing that does not involve a TAU procedure. The process can be described using the same D-MAP tools used to derive \bar{N}_{TAU} . Then, the mean number of TA crossings \bar{N}_{TA} , can be obtained through the results obtained in the Appendix A, but considering a DTMC $\mathbf{\Pi}$ formed just by a TA and its neighboring SCs. In Figure 11 we show a TA with $S_{TA}=3$ and its surrounding SCs. In this case \mathbf{D}_0 is formed by the transitions that occur inside the TA and \mathbf{D}_1 is formed by the transitions that go outside the TA. By properly replacing these new \mathbf{D}_0 and \mathbf{D}_1 in (27), the mean number of TA crossings, \bar{N}_{TA} is obtained. It should be considered that in this case $\mathbf{I}_{mdf} = \mathbf{I}$, in other words, $\mathbf{P}_{fsc} = \mathbf{P}_{isc}$ since the location of the UE does not change inside the TA when, neither, an LU in the LA is performed or a call is received. Therefore,

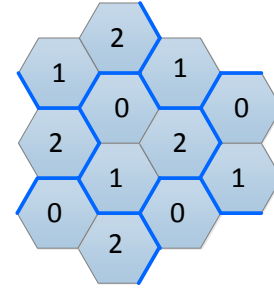


Fig. 11: Diagram to calculate \bar{N}_{TA} for $S_{TA}=3$.

the mean number of LUs to the LA, $\bar{L}\bar{U}_{LA-TA}$ is given by

$$\bar{L}\bar{U}_{LA-TA} = \bar{N}_{TA} - \bar{N}_{TAU}. \quad (4)$$

4.3.3 Paging Probabilities

Here we derive the paging probabilities according to the LU procedure for TALs. From results in Appendix A.3 , it is clear that the probability to find the UE visiting SC j in the actual TAL is given by \mathbf{P}_{fsc} . Its component j , i.e. $P_{fsc,j}$ is the probability to find the UE visiting SC j of the TAL of size $N_c = S_{TA} \cdot S_{TAL}$. Therefore the probability of finding a UE in a given TA, p_{F-TA} is given by

$$p_{F-TA} = \sum_{j \in \Omega} \mathbf{P}_{fsc,j}, \quad (5)$$

where Ω is the set of SCs that belong to the referred TA.

5 DEFINITION OF SIGNALING COSTS

In this section, we define the signaling cost function for the existing 3GPP-based scheme and the two proposed LA-based schemes. The total signaling cost is composed of the location update and the paging costs.

5.1 Tracking Area Update and Location Update Costs

The total cost of performing Tracking Area Updates (TAU), C_{LU-TAU} is given by

$$C_{LU-TAU} = C_{LU-MME} \cdot \bar{N}_{TAU}, \quad (6)$$

where C_{LU-MME} is the cost of performing a single TAU procedure according to the description of Figure 2.

The LA-based schemes perform an LU to the LA whenever a SC or a TA is crossed. The cost of a single LU to the LA is defined as C_{LU-LA} , following the LU procedure described in Figure 5. Therefore, the total cost of LUs for the LA-SC and LA-TA based schemes are, respectively

$$C_{LU-SC} = C_{LU-LA} \cdot \bar{L}\bar{U}_{LA-SC}, \quad (7)$$

$$C_{LU-TA} = C_{LU-LA} \cdot \bar{L}\bar{U}_{LA-TA}. \quad (8)$$

5.2 Paging Cost

The cost of a single paging procedure in 3GPP as shown in Figure 3 is $C_{pag-3GPP}$. In this work, we consider a two step paging scheme for the 3GPP-based solution [8]. In a first attempt, the SCs that belong to the TA or TAs are paged, and in the case of no success, the rest of the SCs of the TAL are paged. Therefore, the total paging cost for the 3GPP-based scheme, $C_{PG-3GPP-based}$ is given by

$$C_{PG-3GPP-based} = C_{pag-3GPP} \cdot p_{F-TA} \cdot N_{sc-c} + C_{pag-3GPP} \cdot (1 - p_{F-TA}) \cdot S_{TA} \cdot S_{TAL}, \quad (9)$$

where N_{sc-c} is the number of SCs in the center of the TAL. In the particular case that the center of the TAL is composed of only one TA, $N_{sc-c} = S_{TA}$.

The paging procedures used by the LA-based schemes follow the sequence shown in Figure 6. The MME pages the Local Anchor through the S1 interface, which identifies the last SC or TA registered and forwards the paging message using the X2 interface to the corresponding SC or TA through the X2 Router. Using $C_{pag-3GPP}$ as a reference, the paging costs for the SC update solution and the TA update solution are, respectively

TABLE 2: Sets of costs for analysis.

Set	$C_{pag-3gpp}$	C_{LU-MME}	C_{LU-LA}
1	1	10	2
2	1	10	3
3	1	10	4
4	1	10	5

$$C_{PG-LA-SC} = 3 \cdot C_{pag-3GPP}, \quad (10)$$

$$C_{PG-LA-TA} = (2 + S_{TA}) \cdot C_{pag-3GPP}. \quad (11)$$

5.3 Total Cost

The total cost for the 3GPP-based scheme and the two proposed LA-based solutions are composed of the total location update cost and paging, and are given by

$$Cost_{3GPP-based} = C_{LU-TAU} + C_{PG-3GPP-based}, \quad (12)$$

$$Cost_{LA-SC} = C_{LU-TAU} + C_{LU-SC} + C_{PG-LA-SC}, \quad (13)$$

$$Cost_{LA-TA} = C_{LU-TAU} + C_{LU-TA} + C_{PG-LA-TA}. \quad (14)$$

6 PERFORMANCE EVALUATION

In this section, we compare our two proposed schemes with the 3GPP-based solution. We evaluate the proposed location management schemes to assess the impact that different parameters have in their performance. In Table 2 four different sets of cost values are defined. We have set the TAU cost to be 10 times the cost of paging procedures as has been consistently used in previous location management works [9], [36],[37]. Unless otherwise stated, the cost set used through this work is 2.

6.1 Random-Walk Mobility

In Figure 12, the location update, paging and total costs for a system with $S_{TA}=12$, $S_{TAL}=7$, and $\gamma=1$ are shown for the 3GPP-based, and the two proposed LA-based solutions as a function of mobility through θ . In this case, $\alpha=1$ is used, and therefore we have a random-walk mobility model. As expected, the total location update cost shown in Figure 12(a) grows with mobility and is lower for the 3GPP-based solution since it only considers TAU procedures, while the LA-based solutions include the updates to the local anchor. On the other hand, in Figure 12(b) the paging is higher for the 3GPP solution since the location of the user is known in a TAL granularity, which in this case has a size of 84 SCs. As expected, for higher mobility values the probability of finding the UE in the center of

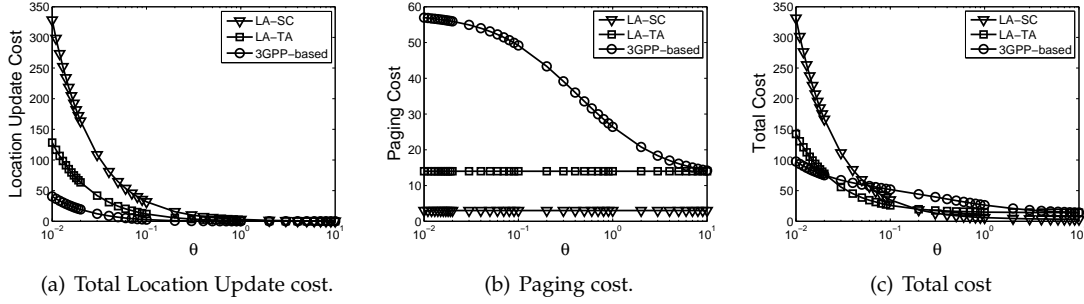


Fig. 12: Costs for system with $\alpha=1, \gamma=1, S_{TA}=12$ and $S_{TAL}=7$.

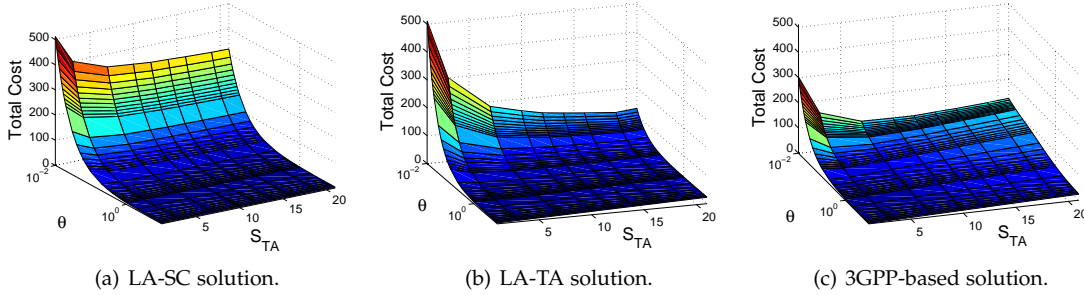


Fig. 13: Total cost for system with $S_{TAL}=7, \alpha=1$.

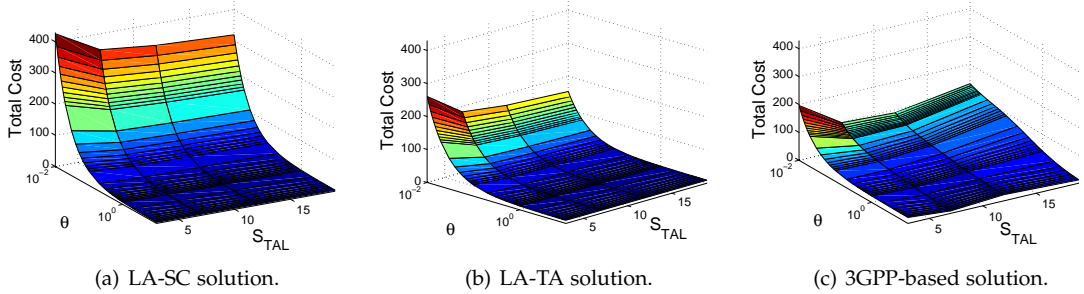


Fig. 14: Total cost for system with $S_{TA}=7, \alpha=1$.

the TAL decreases, and hence the paging cost grows. This variation does not occur with the paging in the LA-based schemes since in these cases the location of the user is known in a fixed basis (SC or TA). According to Figure 12(c), for low mobility values the LA-SC scheme has the lowest total cost, because by having the lowest paging cost, at this point the influence of location updates is not too high. However, as mobility grows, the total cost for this scheme rapidly surpasses the other two solutions. In this scenario, the LA-TA scheme has the lowest total cost for θ between 0.02 and 0.2. For $\theta < 0.02$, the 3GPP-based solution per-

forms better. Therefore, for high mobility values, the signaling overhead reduction in paging achieved by the LA-based solutions is not enough to compensate for the location updates to the local anchor. In fact, when $\theta=0.01$, the LA-TA scheme total cost is over 50% higher than the one obtained by the 3GPP based solution. However, UEs' location precision is 7 times higher than the 3GPP-based solution for the LA-TA scheme and 84 times for the LA-SC scheme. In Figure 13 the total cost for the three solutions is shown as a function of θ and S_{TA} , for a system with $S_{TAL}=7, \gamma=1$ and $\alpha=1$. For the LA-SC scheme

in Figure 13(a), the total cost grows with mobility and decreases as S_{TA} grows. This reduction in the total cost is associated with a reduction in TAU procedures, since S_{TA} does not affect $\bar{L}U_{LA-SC}$. Although this scheme reaches the finest granularity independently of the value of S_{TA} and S_{TAL} , the impact of the LUs to the LA is too significant in the total cost. For the LA-TA scheme, Figure 13(b), some improvement can be achieved through S_{TA} adjustments. Clearly, the total cost monotonically increases with mobility. However, by fixing θ , increasing S_{TA} will first decrease the total cost because the LUs to the LA and TAU procedures are reduced, and then will increase the total cost because the paging (proportional to S_{TA}) will overcome the LU reduction. Therefore, an optimal value for S_{TA} can be found for each θ , and this value is higher as mobility increases. A similar behavior occurs in the 3GPP solution shown in Figure 13(c). In this case, the reduction in TAU procedures achieved by increasing S_{TA} is rapidly countered by the increase in paging, which is proportional to $S_{TA} \cdot S_{TAL}$.

In Figure 14 the total cost for the three solutions is shown as a function of θ and S_{TAL} , for a system with $S_{TA}=7$, $\gamma=1$ and $\alpha=1$. As expected, the total cost for the LA-SC solution grows with mobility and S_{TAL} as can be seen in Figure 14(a). The same behavior is seen for the LA-TA solution, Figure 14(b), where the cost reduction achieved by increasing S_{TAL} is an effect of the reduction of TAU procedures, since $\bar{L}U_{LA-TA}$ is not affected. On the other hand, increasing S_{TAL} has the same effect than increasing S_{TA} on the 3GPP solution. The cost function grows with mobility and first decreases as S_{TAL} grows because of a TAU procedures reduction, but then grows again due to the increase in paging. The most interesting characteristic of Figure 14(c) is the influence of the shape of the TAL in the cost. This is more evident for low mobility, when changing S_{TAL} from 3 to 7 reduces the total cost, but increasing S_{TAL} from 7 to 12 causes a new slight reduction. However, this differences diminish as mobility increases.

6.2 Mobility Pattern Variations

Until now, the main characteristics of the three solutions have been described for variations of θ , S_{TA} and S_{TAL} when a random-walk model is used. However, in this subsection we evaluate the impact of changes in the mobility pattern for our two proposed LM solutions and the 3GPP-based solution.

First, let us evaluate the mean number of TAU procedures \bar{N}_{TAU} , when a central and adaptive TAL configurations are used. In Figure 15, \bar{N}_{TAU} is evaluated for the two TAL configuration methods as α grows from 1 to 50, orientation is 2, $S_{TAL}=7$, $\gamma=1$, $\theta=0.1$, and

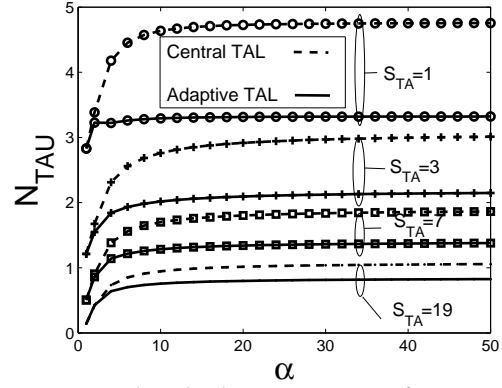


Fig. 15: Central and adaptive TAL configuration comparison.

four different values of S_{TA} . Clearly, the adaptive TAL configuration reduces \bar{N}_{TAU} for every case when $\alpha > 1$, since the adaptive solution is the same as the central solution when the random-walk model ($\alpha=1$) is used. This reduction is higher as S_{TA} is lower, and for the lowest size, $S_{TA}=1$, a reduction of 30% is achieved. When $S_{TA}=19$, the achieved reduction is of 21%. It should be noted that TAL configuration is common for the three presented LM solutions.

In order to compare the impact of mobility patterns, let us define the cost reduction of the LA-based solutions in relation to the 3GPP solution Λ_{LA-SC} and Λ_{LA-TA} as

$$\Lambda_{LA-SC} = \frac{\min(Cost_{LA-SC}) - \min(Cost_{3GPP-based})}{\min(Cost_{3GPP-based})}, \quad (15)$$

$$\Lambda_{LA-TA} = \frac{\min(Cost_{LA-TA}) - \min(Cost_{3GPP-based})}{\min(Cost_{3GPP-based})}, \quad (16)$$

where the \min function searches for the combination of S_{TA} and S_{TAL} for a fixed θ that minimizes the cost for each scheme.

In Figure 16, the total cost reduction of the two LA-based schemes in relation to the 3GPP-based scheme for a system with $S_{TA}=7$, $\gamma=1$, orientation=2 and $\alpha=10$ when θ goes from 0.01 to 10 is shown. As it was seen in previous scenarios, the LA-SC scheme works better for high values of θ , while the LA-TA is better for low values of θ . An important fact of the LA-TA scheme is that it achieves a maximum total cost reduction when $\theta=0.8$. For lower values of θ the cost reduction is shorter, and in fact when $\theta=0.018$, the total cost of the LA-TA scheme is slightly higher than the 3GPP-based solution. However, this solution works for a high range of θ values while at the same time maintains the location granularity fixed, since $S_{TA}=7$. On the other hand, the cost of the LA-SC scheme is

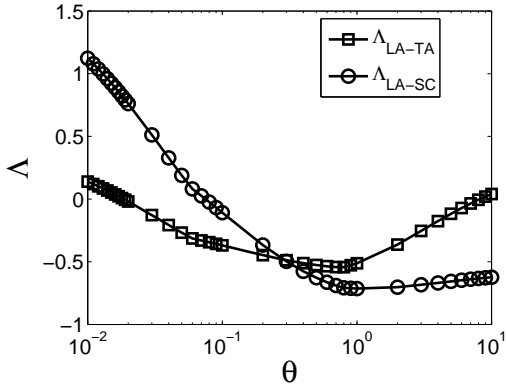


Fig. 16: Cost reduction for a system with $S_{TA}=7$, $\gamma=1$, $\alpha=10$, orientation=2.

higher than the cost of the 3GPP-based solution for any $\theta < 0.08$.

In Figure 17 the total cost reduction of the two LA-based schemes in relation to the 3GPP-based scheme for a system with $S_{TA}=7$, $\gamma=1$, orientation=2 and $\alpha=10$ for different cost sets as θ goes from 0.01 to 10 are shown. Clearly, increasing the cost of location updates to the local anchor reduces the range of θ values where the LA-based solutions have a lower total cost. In 17(a), when C_{LU-LA} grows from 2 to 5, the maximum $1/\theta$ for which the LA-SC is valid is reduced from 26 to 6. However, as it was previously stated, the LA-SC scheme is only suited for high values of θ . For the LA-TA solution shown in Figure 17(b), the maximum possible $1/\theta$ when C_{LU-LA} grows from 2 to 5, is reduced from 120 to 22. Therefore, it is necessary to maintain C_{LU-LA} as low as possible.

In Figure 18 the variance of the residence time in a SC is modified through the parameter γ , for a system with $S_{TA}=7$, orientation=2 and $\alpha=10$. The cost reduction of the LA-SC and the LA-TA schemes for several values of θ are shown in Figures 18(a) and 18(b) respectively. In Figure 18(a) it can be seen that the performance of the LA-SC solution is affected for high values of θ when the variance is diminished, but on the other hand, for very low values of γ (high variance), the LA-SC scheme reduces the total cost for high mobility values (low θ). On the other hand, the LA-TA solution in Figure 18(b) is not affected when variance is reduced for low θ (high mobility). However, as variance grows, performance is affected for low values of θ , reducing the range of useful mobility values.

6.3 Mobility Traces Considerations

In [11], the Call Data Records (CDRs) from 3 different cities in USA are analyzed to obtain the mobility patterns of users. Two important conclusions for voice

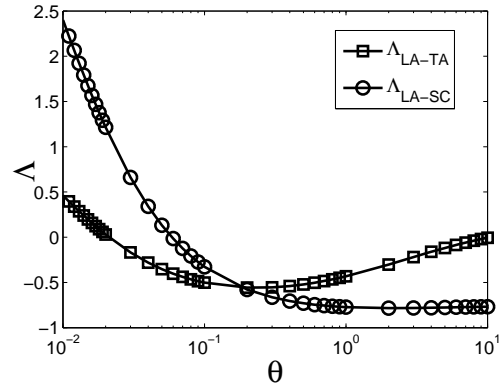


Fig. 19: Cost reduction for a system with $\alpha=1$, $\gamma=1$, $S_{TA}=12$ and $S_{TAL}=7$.

users are obtained: First, a large portion of users (96%) visit a low number of cells (low mobility) in a fixed period (< 40 cells/day). Also, these users receive very few calls ($\lambda_{c,s} \approx 0.52$ calls/day). Second, while only 4% of users visit more than 40 cells per month, they receive a high volume of calls ($\lambda_{c,f} \approx 7.68$ calls/day). Therefore, there are two types of voice users: (i) a high percentage of low mobility/low traffic users, and (ii) a low percentage of high mobility/high traffic users.

With the data provided in [11], it is not possible to define the rate of cell crossings per day. However, we can infer that for users of the first type, $\lambda_{m,s} < 40$ (cells/day). With this in mind, and using $\lambda_{c,s}$ as provided above, we define the range of θ values of interest for low mobility users as $\theta_s = \lambda_{c,s} / \lambda_{m,s}$. Hence, $\theta_s > 0.013$. In Figure 19, we evaluate the total cost reduction of the two proposed location management schemes against the 3GPP-based solution, for a system with $S_{TA}=12$, $S_{TAL}=7$, $\gamma=1$ and $\alpha=1$, i.e., random-walk. It can be seen that for the lowest value of interest, $\theta=0.013$, the 3GPP-based solution is the best. Only when θ reaches 0.03, the LA-TA scheme is better, and this continues for the whole range of θ_s ($\lambda_m < 17$ cells/day). On the other side, the LA-SC scheme only outperforms the 3GPP-based solution when θ reaches 0.06 ($\lambda_m < 9$ cells/day). Therefore, the proposed solutions perform better for users with the lowest mobility.

According to the traces defined in [12], the majority of the movements of high traffic users, are done in long distances, with trajectories that cover on average 40 km. This type of movements are represented in our mobility model when $\alpha > 1$. Using the data from [11], we can infer that for high mobility users, $\lambda_{m,f} > 40$ (cells/day). Hence, the range of θ values for this type of users is $\theta_f = \lambda_{c,f} / \lambda_{m,f} < 0.19$. In Figure 16, the cost reduction of the two proposed schemes for a system with $S_{TA}=7$, $\gamma=1$, $\alpha=10$ and orientation = 2

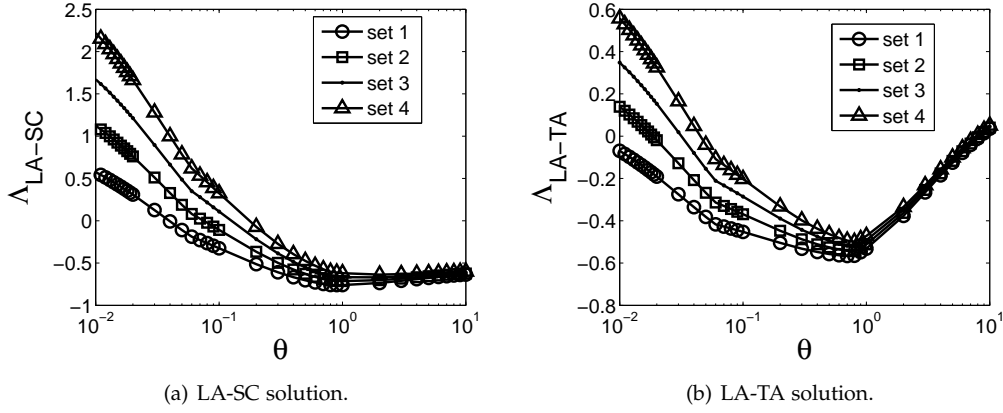


Fig. 17: Total cost reduction for system with $S_{TA}=7$, $\gamma=1$, orientation=2 and $\alpha=10$.

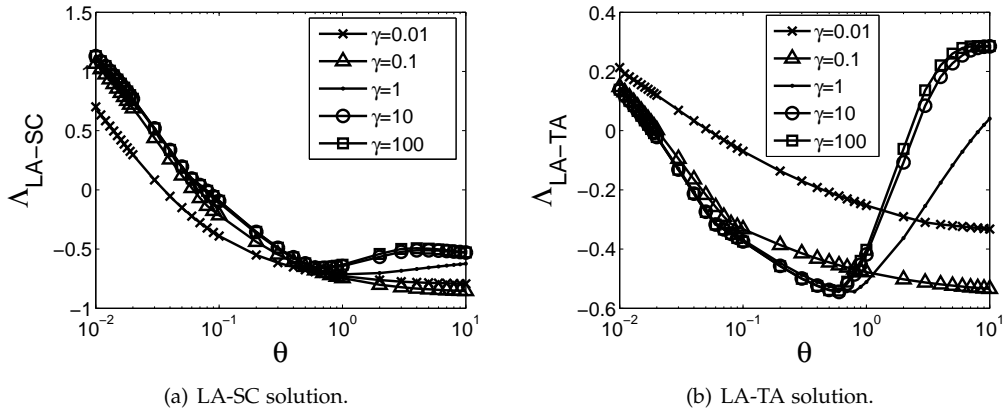


Fig. 18: Total cost reduction for system with $S_{TA}=7$, set=2, orientation=2 and $\alpha=10$.

is shown. For the case of $\lambda_{m,f}=120$ (cells/day), ($\theta=0.064$), the total cost reduction of the LA-TA scheme is of 35%, and this reduction reaches 45 % when $\theta=0.19$. The LA-SC scheme is effective for a smaller range of θ , since it only achieves a total cost reduction when $\lambda_{m,f} < 100$ (cells/day). Therefore, the proposed solutions are effective for the most relevant range of high mobility users.

7 CONCLUSION

In this work, we proposed two new location management methods for small cells to reduce signaling overhead in the MME while achieving an accurate location of UEs. The proposed methods use a local anchor in the SC network to keep a record of UEs' locations in a SC or TA basis. Given that the local anchor changes with each UE, we managed to distribute the processing load associated with location updates. Also, by

registering UEs' locations more often, the proposed schemes reduce the paging signaling cost in the MME. Communication among SCs is done through the X2 interface, and an X2 router is introduced for scalability purposes. In order to include the mobility patterns of users, we proposed an adaptive Tracking Area List setting method that reduces the frequency of location updates. For analytical purposes, we developed a 2D mobility model which considers several TA and TAL sizes, UEs' movement patterns and SCs' residence time characteristics. Through this model, we derived analytical expressions for the signaling cost of our two proposed schemes and an existing 3GPP-based scheme. We compared the three solutions for different scenarios and the results showed that our proposed schemes are able to reduce the signaling overhead in relation to the existing 3GPP standard solution. By means of analysis of the obtained results, we were able

to establish the impact that several parameters have over the proposed solutions.

ACKNOWLEDGMENT

This work has been supported by European Commission under the FP7 S2EuNet project and the Spanish Government through project TIN2010-21378-C02-02

REFERENCES

- [1] Ericsson Labs, "Heterogeneous networks: Meeting mobile broadband expectations with maximum efficiency", *Ericsson White Paper*, 2012.
- [2] Femto Forum, "Femtocells- natural solution for offload, a femto forum topic brief", *Femto Forum*, 2010.
- [3] Metis Consortium, "Scenarios, requirements and KPIs for 5G mobile and wireless system", FP7-ICT-317669-METIS deliverable D1.1, 2013
- [4] 3GPP TS 23.401 V12.2.0 (2013-09).
- [5] B. Hajek, K. Mitzel, and S. Yang, "Paging and registration in cellular networks: Jointly optimal policies and an iterative algorithm", *IEEE Transactions on Information Theory*, Vol. 54, n. 2 pp. 608–622, February 2008.
- [6] C. Rose, and R. Yates, "Minimizing the average cost of paging under delay constraints", *Wireless Networks*, Vol. 1, n. 2, pp 211–219, June 1995.
- [7] I. Akyildiz, J. Ho and Y. Lin., "Movement-based location update and selective paging for PCS networks", *IEEE/ACM Transactions on Networking*, Vol 4. n.4 pp. 629–638 August 1996.
- [8] R. Liou, Y. Lin, and S. Tsai, "An Investigation on LTE Mobility Management", *IEEE Transactions On Mobile Computing*, vol. 12, no.1, pp. 166-176, January 2013.
- [9] J. Ferragut and J. Mangues-Bafalluy, "A Self-Organized Tracking Area List Mechanism for Large-Scale Networks of Femtocells", in *Proceedings of IEEE International Conference on Communications (ICC 2012)*, 10 - 15 June, 2012, Ottawa (Canada).
- [10] S. Modarres Razavi, D. Yuan, F. Gunnarson and J. Moe, "Exploiting Tracking Area List for Improving Signaling Overhead in LTE", *Proceedings of Vehicular Technology Conference 2010*.
- [11] H. Zang and J. Bolot, "Mining Call and Mobility Data to Improve Paging Efficiency in Cellular Networks", in *proceedings of the 13th annual international conference on Mobile computing and networking, MobiCom 07*, pp. 123–134, 2007
- [12] A. Sridharanm and J. Bolot, "Location Patterns of Mobile Users : A Large-Scale Study", in *proceedings of IEEE INFOCOM*, 2013.
- [13] Alcatel-Lucent, "The Impact of Small Cells on MME Signaling", *Alcatel-Lucent, Application Note*, October 2013.
- [14] J. Ferragut, J. Mangues-Bafalluy, J. Nunez-Martinez and F. Zdarsky, "Traffic and Mobility Management in Networks of Femtocells", *Mobile Networks and Applications*, Vol 17, Issue 5, October 2012, pp. 662–673.
- [15] 3GPP TS 36.420 V11.0.0 (2012-10).
- [16] J. Ho and I. Akyildiz, "Local Anchor Scheme for Reducing Signaling Costs in Personal Communications Networks", *IEEE/ACM Transactions on Networking*, vol. 4, no. 5, pp. 709–725, 1996.
- [17] 3GPP TR 37.803 V11.1.0 (2013-06).
- [18] V. Casares-Giner and J. Mataix-Oltra, "Global Versus Distance-Based Local Mobility Tracking Strategies: A Unified Approach", *IEEE Transactions on Vehicular Technology*, vol. 51, no. 3, pp. 472–485, 2002
- [19] H-W Hwang, M-F Chang, and C-C Tseng, "A Direction-Based Location Update Scheme with a Line-Paging Strategy for PCS networks", *IEEE Communications Letters*, Vol. 4, n. 5, pp. 149-151, May 2000.
- [20] D. Pacheco-Paramo, I. Akyildiz and V. Casares-Giner, "X2-Interface-Based Location Management for Small Cell Networks", in *proceedings of GLOBECOM*, 2013.
- [21] V. Casares-Giner, V. Pla, and P. Escalle-Garcia, "Mobility Models for Mobility Management", *Next Generation Internet*, LNCS 5233, pp. 716–745, Springer-Verlag, 2011.
- [22] Small Cell Forum, Release Four, Document 104.04.01 Urban. Overview. June 2014.
- [23] Small Cell Forum, Release Four, Document 098.04.01 Urban Small Cells in the Real World. Case Studies. June 2014.
- [24] E. Alonso, K. S. Meier-Hellstern and G. P. Polini "Influence of cell geometry on handover and registration rates in cellular and universal personal telecommunication networks". In *Proceedings of the 8th ITC Specialist Seminar on Universal Personal Telecommunications*. pp. 261-260. 1992.
- [25] S. Okasaka, S. Onoe, S. Yasuda, and A. Maebara, "A new location updating method for digital cellular systems", in *Proceedings 41st Annual Conference VTS*, May 1991, pp. 345-350.
- [26] P. Garcia Escalle, V. Casares-Giner, J. Mataix-Oltra, "Reducing Location Update and Paging Costs in a PCS Network", *IEEE Transactions on wireless communications*, vol. 1, no.1, pp.200–209, 2002.
- [27] S. Yang, Y. Lin, and Y. Lin, "Performance of Mobile Telecommunications Network With Overlapping Location Area Configuration", *IEEE Transactions on Vehicular Technology*, Vol. 57, n. 2 pp. 1285–1292, March 2008.
- [28] R. Liou and Y. Lin, "Mobility management with the central-based location area policy", *Computer Networks*, vol. 57, no.4, pp. 847-857, March 2013.
- [29] M. Ficek and L. Kenel, "Inter-Call Mobility Model: A Spatio-temporal Refinement of Call Data Records Using a Gaussian Mixture Model", in *proceedings of IEEE INFOCOM*, 2012.
- [30] R. Liou, Y. Lin, Tsai S. "An Investigation on LTE Mobility Management", *IEEE Transactions on Mobile Computing*, Vol. 12 no 1, 2013.
- [31] Ronald W. Wolff, "Poisson Arrivals See Time Averages", *Operations Research*, Vol. 30, No. 2. (Mar. - Apr., 1982), pp. 223-231.
- [32] D. M. Lucantoni, "The BMAP/G/1 queue: a tutorial ", *Models and techniques for performance evaluation of computer and communication systems*, pp. 330-358, Springer-Verlag, 1993.
- [33] F. Machihara, "Completion time of service unit interrupted by a PH-Markov renewalcustomers and its applications", in *proceedings of the 12th ITC*, paper 5.4B 5.1-5.8. 1988.
- [34] F. Machihara, "A preemptive priority queue with non renewal inputs. Matrix-analytic methods in stochastic models", *Lecture notes in pure and applied mathematics*, Ed. Chkravarthy and Alfa, Dekker, 1997.
- [35] M. M. Zonoozi and P. Dassanayake, "User Mobility Modeling and Characterization of Mobility Patterns", *IEEE Journal on Selected Areas on Communications*, Vol. 15, No.7, pp. 1239-1252, Sep- 1997.
- [36] Y. Tseng, L. Chen, M. Yang and J. Wu, "A stop-or-move mobility model for PCS networks and its location-tracking strategies", *Computer Communications*, Vol. 26, Issue 12, 21 pp. 1288-1301, Jul-2003.
- [37] A. Chandra and K. Mal, "Genetic Algorithm Based Optimization for Location Update and Paging in Mobile Networks", in *proceedings of Asian Applied Computing Conference, AACC' 04*, pp. 222-231, 2004.